Oncogene (2007) 26, 7508–7516

www.nature.com/onc

ORIGINAL ARTICLE

Significance of HIF-1-active cells in angiogenesis and radioresistance

H Harada[1,2], S Kizaka-Kondoh[1,3], G Li[1,5], S Itasaka[1], K Shibuya[1], M Inoue[4] and M Hiraoka[1]

[1]*Department of Radiation Oncology and Image-Applied Therapy, Kyoto University Graduate School of Medicine, Kyoto, Japan;* [2]*Nano-Medicine Merger Education Unit, Kyoto University, Kyoto, Japan;* [3]*COE Formation for Genomic Analysis of Disease Model Animals with Multiple Genetic Alterations, Kyoto University Graduate School of Medicine, Kyoto, Japan and* [4]*Department of Biochemistry, Osaka Medical Center for Cancer and Cardiovascular Diseases, Osaka, Japan*

Human solid tumors contain hypoxic regions that have considerably lower oxygen tension than the normal tissues. Hypoxia offers resistance to radiotherapy and anticancer chemotherapy, as well as predispose to increased tumor metastases. Furthermore, hypoxia induces hypoxia-inducible factor-1 (HIF-1), which in turn increases tumor angiogenesis. Thus, eradication of HIF-1-active/hypoxic tumor cells is very important for cancer therapy. We have previously reported that procaspase-3 fused with a von Hippel–Lindau (VHL)-mediated protein destruction motif of alpha subunit of HIF-1 (HIF-1α) containing Pro564, named TAT-ODD-procaspase-3 (TOP3), specifically induced cell death to hypoxic cells *in vivo* as well as *in vitro*. We now report that TOP3 also eradicates the radiation-induced HIF-1-active tumor cells. HIF-1 activity in the xenografts of human tumor cells, which express luciferase under the transcriptional control of HIF-1, were monitored and quantified daily with an *in vivo* bioluminescence photon-counting device. HIF-1 activity in tumors was more rapidly increased by ionizing radiation (IR) compared to untreated tumors. TOP3 efficiently decreased the HIF-1-activity in irradiated tumors as well as unirradiated ones, indicating TOP3 eradicated tumor cells with HIF-1-activity induced by IR as well as hypoxia. Eradication of HIF-1-active/hypoxic cells in the xenografts during irradiation exhibited significant suppression in angiogenesis and strong enhancement in a long-term growth suppression of tumor xenografts. These results further strengthen the argument that HIF-1-active/hypoxic cells play crucial roles in angiogenesis and radioresistance.
Oncogene (2007) **26,** 7508–7516; doi:10.1038/sj.onc.1210556; published online 11 June 2007

Keywords: tumor hypoxia; angiogenesis; HIF-1; radiotherapy

Correspondence: Dr S Kizaka-Kondoh, Department of Radiation Oncology and Image-applied Therapy, Kyoto University Graduate School of Medicine, 54 Kawahara-cho, Shogoin, Sakyo-ku, Kyoto 606-8507, Japan.
E-mail: skondoh@kuhp.kyoto-u.ac.jp
[5]Current address: Cancer Center, The General Hospital of Chinese People's Armed Police Forces, Yongding Road 69, Haidian District, Beijing 100039, China.
Received 7 March 2007; revised 18 April 2007; accepted 25 April 2007; published online 11 June 2007

Introduction

Reduced oxygen tension far below physiological levels is a characteristic of solid tumors (Vaupel *et al*., 1989; Harris, 2002; Brown and Wilson, 2004). Polarographic needle electrode analysis and immunohistochemical analysis with antibodies against hypoxia markers have demonstrated that solid tumors contain severely hypoxic regions, in which pO_2 values are less than 10 mmHg (Höckel *et al*., 1993; Raleigh *et al*., 1998). Because oxygen has the highest affinity for electrons among any molecule in the cell, it reacts rapidly with unpaired electrons of free radicals in irradiated DNA, thereby aggravating radiation damage (Brown, 1999; Vaupel, 2001). Therefore, cytocidal effects of ionizing radiation (IR) are severely compromised under low oxygen tension, making hypoxia a critical limitation for the success of radiotherapy.

Hypoxia-inducible factor-1 (HIF-1) is expressed in hypoxic tumor cells. In addition, HIF-1 is also induced transiently in tumors following radiotherapy in response to the reoxygenation stress, and this induction peaked at around 48 h after irradiation (Moeller *et al*., 2004). HIF-1 transactivates various hypoxia-responsive genes, which confer malignant properties to tumors such as apoptosis resistance, enhanced tumor growth, invasion and metastasis (Semenza, 2003). In addition, HIF-1 activates proangiogenic cytokines such as vascular endothelial growth factor (VEGF) and platelet-derived growth factor, which confer radiation resistance to endothelial cells as well as increase the proliferation and regrowth of tumor blood vessels (Gorski *et al*., 1999; Geng *et al*., 2001; Abdollahi *et al*., 2003; Moeller *et al*., 2004). Neovascularization is a particularly important contribution of HIF-1 to the survival and regrowth of tumors after irradiation (Abdollahi *et al*., 2003). Thus, hypoxia impacts tumor radioresponsiveness not only in altering the physicochemical properties of radiation-induced DNA damage, but also in activation of pro-angiogenic genes, which are crucial for the survival and proliferation of tumors under these adverse conditions.

HIF-1 is a heterodimer composed of α and β subunits, and HIF-1α is regulated in an oxygen-dependent manner at the post-translational level (Semenza and Wang, 1992; Huang *et al*., 1998; Kallio *et al*., 1999; Semenza, 2003). In normoxia, HIF-1α is hydroxylated at

its proline residues of the oxygen-dependent degradation (ODD) domain by prolyl hydroxylases (Bruick and McKnight, 2001; Epstein *et al*., 2001). The modification accelerates the interaction of HIF-1α with the von Hippel–Lindau (VHL) tumor suppressor protein, resulting in the rapid ubiquitination and subsequent degradation of HIF-1α by the 26S proteasome (Cockman *et al*., 2000; Kamura *et al*., 2000; Ohh *et al*., 2000; Tanimoto *et al*., 2000).

In order to eradicate HIF-1α-expressing hypoxic cells, we have developed TOP3 (TAT-ODD-procaspase-3), a fusion protein with three domains (Figure 1) (Harada *et al*., 2002, 2005, 2006; Kizaka-Kondoh *et al*., 2003; Inoue *et al*., 2004). The PTD is derived from the protein-transduction domain (PTD) of the human immunodeficiency virus type-1 tat protein (Schwarze *et al*., 1999) and efficiently delivers TOP3 to any tissue *in vivo*. The ODD domain contains a VHL-mediated protein destruction motif of human HIF-1α protein and confers hypoxia-dependent stabilization to TOP3 (Harada *et al*., 2006). Procaspase-3 is the proenzyme form of human caspase-3 (Fernandes-Alnemri *et al*., 1994) and confers potential cytocidal activity to TOP3. While TOP3 effectively target hypoxic cells, it does not directly affect the normoxic tumor cells (Harada *et al*., 2005). On the other hand, IR effectively targets normoxic cells but is less effective to hypoxic cells (Brown, 1999; Vaupel, 2001). Thus, we expect that combination of TOP3 and IR would improve the outcome of antitumor treatment.

Here we demonstrate that the combination of TOP3 and IR efficiently reduced tumor cells with HIF-1 activity induced by both hypoxia and irradiation, leading to long-term suppression of tumor growth and angiogenesis.

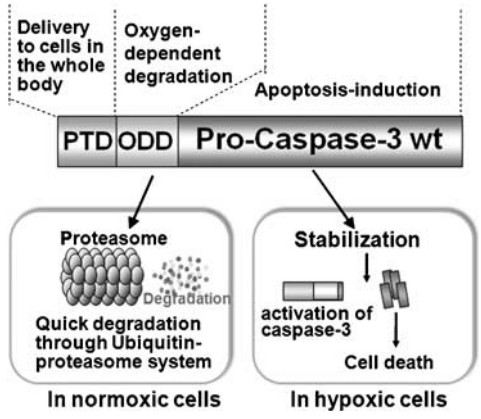

Figure 1 Schematic of structure and domain function of TOP3. TOP3 consists of three domains, which function as drug delivery, oxygen-dependent protein degradation and cell killing. The protein-transduction domain (PTD) enables the fusion protein to diffuse and enter the cell. The stability of TOP3 is regulated by the same mechanism as HIF-1α through the oxygen-dependent degradation (ODD) domain. The procaspase-3 can be activated under hypoxic conditions and induce apoptosis in hypoxic tumor cells.

Results

IR increases HIF-1 activity

Because stabilization of TOP3 is regulated by the same mechanism as HIF-1α (Harada *et al*., 2006), TOP3 has potential cytosical activity to HIF-1-active cells. Thus, we first examined change in HIF-1 activity in the xenografts during the treatment with IR. HIF-1-driven luciferase activity in HeLa/5HRE-Luc xenografts on the right leg was monitored daily with and without irradiation with 10 Gy. We used this dose because the growth-suppressive effect of TOP3 in combination with 5 Gy IR was less clear, while 20 Gy IR alone was effective enough to remove tumors almost completely and thus the effect of TOP3 was not assessed (data not shown). In the unirradiated animals, HIF-1 activity gradually increased as tumors grew over the observation period (Figure 2a, upper panels and Figure 2b), indicating the total number of hypoxic tumor cells in xenografts increase as tumors grow. With irradiation,

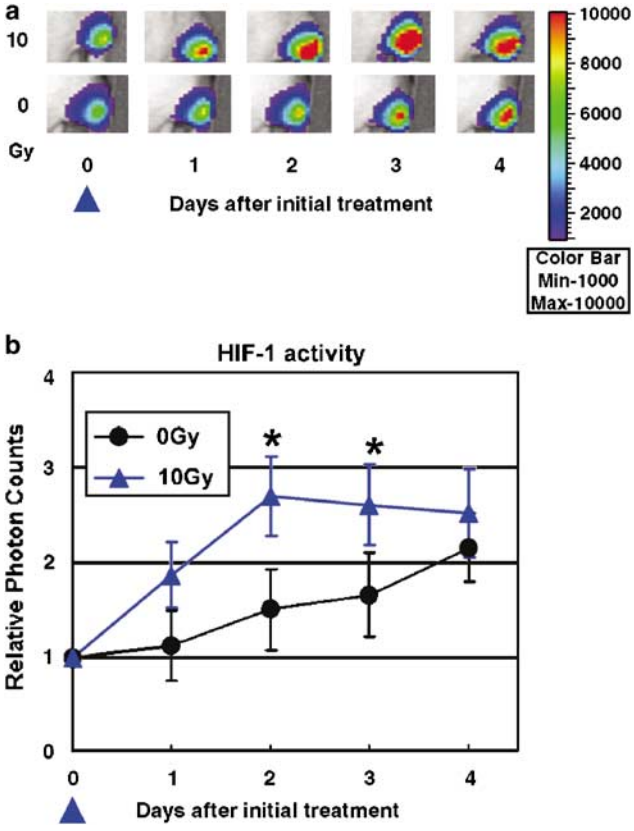

Figure 2 Increase of intratumoral hypoxia-inducible factor-1 (HIF-1) activity by irradiation. Mice ($n=5$ for each group) were transplanted with HeLa/5HRE-Luc cells in the right hind leg. The tumor-bearing mice were treated with local irradiation of xenografts with 0 or 10 Gy on day 0 (blue arrowhead). Change in the intratumoral HIF-1 activity was monitored using bioluminescence (photons/sec) every day with the IVIS photon-counting system. (**a**) A mouse with representative images during the observation period was chosen from the unirradiated (0 Gy) and the 10 Gy-irradiated groups and shown in. (**b**) Photon counts from the xenografts irradiated with 0 and 10 Gy on each day were divided by the corresponding photon counts on day 0 and indicated as relative photon counts. $^*P<0.05$.

HIF-1 activity increased significantly more rapidly for 2 days after irradiation (Figure 2a, lower panels and Figure 2b; $P<0.05$).

Suppression of both hypoxia- and irradiation-induced HIF-1 activities by TOP3

To investigate whether these tumor cells expressing HIF-1 after IR can be target of TOP3, we next examined the antitumor effect of the combination with IR and TOP3. For this purpose, we divided tumor-bearing mice to four groups (buffer, TOP3, IR and TOP3 and IR) and examined effects of monotherapies and the combination therapy on intratumoral HIF-1 activity. When TOP3 was intraperitoneally (i.p.) injected in mice carrying HeLa/5HRE-Luc xenografts on day 0, day 1 and day 2 (Figure 3a), the intratumoral HIF-1 activity was significantly decreased by day 2 (Figure 3a, lower panels and Figure 3b; $P<0.01$). In contrast, HIF-1 activity in buffer-treated HeLa/5HRE-Luc xenografts continuously increased over the observation period (Figure 3a, upper panels and Figure 3b).

Immunohistochemical analysis using an anti-luciferase antibody confirmed that the luciferase protein induced by HIF-1 was localized in the similar region detected by a hypoxia marker, pimonidazole, in untreated xenografts (Figure 3c). In our previous study, the quantitative correlation was demonstrated between the level of HIF-1α expression and the luciferase activity (Harada *et al*., 2005). In the TOP3-treated tumors, HIF-1-induced luciferase and pimonidazole-binding proteins were barely detected (Figure 3c), confirming that TOP3 eliminated HIF-1-active hypoxic cells and reduced the cells reactive with pimonidazole (Harada *et al*., 2005).

In the tumors given IR alone on day 2, HIF-1 activity increased by threefold 2 days after irradiation (Figure 4a, upper panels and Figure 4b). The fold increase of HIF-1 activity of irradiated tumors vs unirradiated tumors from day 2 to day 4 (3.6 vs 2.1, Figures 3b and 4b) was almost identical to the one in Figure 2b (2.5 vs 1.5). When treated with TOP3 for 3 consecutive days from day 0 and irradiated on day 2, the intratumoral HIF-1 activity remained low (approximately threefold of the one on day 0) on day 4 (Figure 4a, lower panels and Figure 4b) and was comparable to the one treated with buffer only on day 4, which was also approximately threefold of the one on day 0 (Figure 3b). This indicated that TOP3 effectively inhibited HIF-1 induced by hypoxia as well as IR.

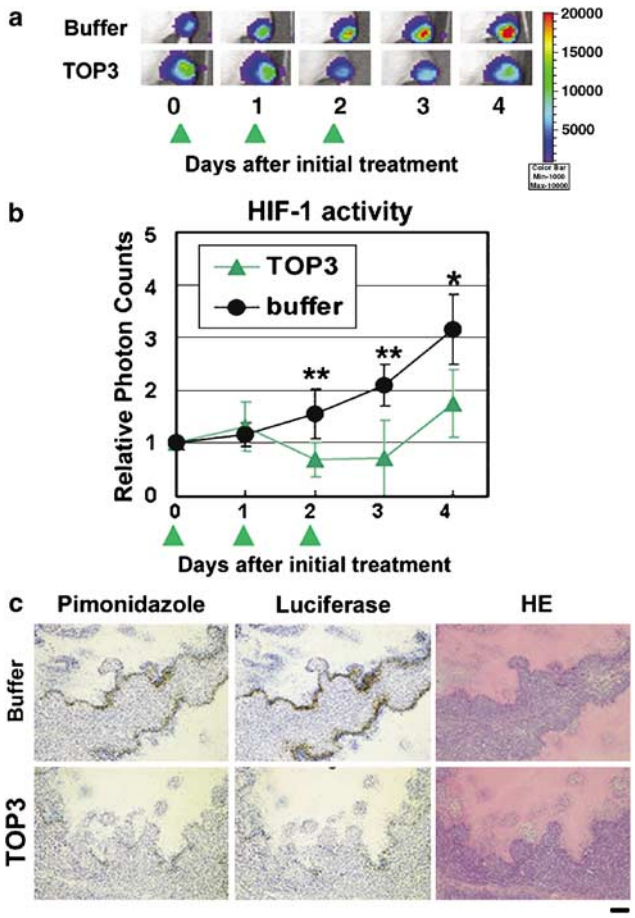

Figure 3 Reduction of hypoxia-induced hypoxia-inducible factor-1 (HIF-1) activity by TAT-ODD-procaspase-3 (TOP3) treatment. Mice ($n=5$ for each group) were transplanted with HeLa/5HRE-Luc cells in the right hind leg. The tumor-bearing mice were treated with local irradiation of xenografts with buffer or TOP3 on day 0, 1 and 2 (green arrowheads). The change in intratumoral HIF-1activity was monitored as described in the legend to Figure 2. (**a**) A mouse with representative images during the observation period was chosen form the control (buffer) and TOP3-treatment (TOP3) groups and shown in. (**b**) Photon counts from the xenografts on each day were divided by the corresponding photon counts on day 0 and indicated as relative photon counts. $*P<0.01$; $**P<0.005$. (**c**) Buffer- or TOP3-treated xenografts were surgically excised on day 2 and used for immunohistochemical analysis with anti-pimonidazole antibody (Pimonidazole), anti-luciferase antibody (Luciferase) and hematoxylin and eosin (HE). Bar = 100 μm.

Suppression of long-term tumor growth by the combination of TOP3 and IR

Next we examined effects of monotherapies and the combination therapy on tumor growth. The growth of HeLa/5HRE-Luc xenografts was significantly but temporarily suppressed by TOP3 alone over a 12-day period (Figure 5a; $P<0.05$ over none). The growth of tumors treated by IR (10 Gy) alone was significantly suppressed starting from 1 week after irradiation (Figure 5a; $P<0.01$ over none). During a 14-day observation period, the combination treatment did not have a significantly greater effect than IR alone. However, when the observation was extended to 80 days, the combination treatment was much more effective (Figure 5b). The days required for the tumor volume to increase threefold (tripling time) was 11.1 ± 2.2 days for the buffer-treated animals and 13.6 ± 3.2 days for the TOP3 alone. This small difference due to TOP3 alone was due to the low dose used. This gave us an opportunity to precisely analyse the efficacy of the combination treatment with TOP3 and radiotherapy. The tripling time was 41.6 ± 5.5 days for the IR alone, while that for the combination treatment was 75.7 ± 11.6 days. Thus, a large enhancement was observed for the combination treatment

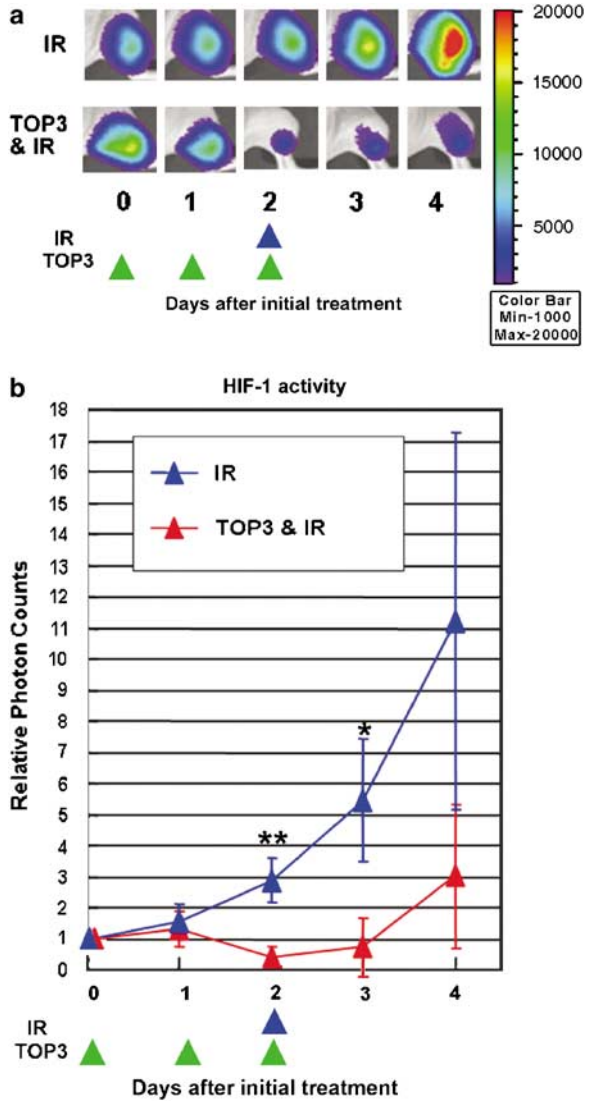

Figure 4 Reduction of the intratumoral hypoxia-inducible factor-1 (HIF-1) activity by TAT-ODD-procaspase-3 (TOP3) and ionizing radiation (IR). Tumor-bearing mice ($n=5$ for each group) with HeLa/5HRE-Luc xenografts in the right hind leg were irradiated with 10 Gy on day 2 (blue arrowhead). Mice of the TOP3 and IR group were additionally treated with TOP3 on day 0, 1 and 2 (green arrowheads). (**a**) A mouse with representative images during the observation period was chosen form the IR-alone group (upper panel) and the TOP3 and IR group (lower panel) and shown in. (**b**) The intratumoral HIF-1 activity was monitored as described in the legend to Figure 2 and presented in the graph. $*P<0.01$; $**P<0.005$.

which delayed tumor growth by 1.8-fold over IR alone. We also tested the combination treatments on CFPAC-1 xenografts and similar results were obtained (Figures 5c and d).

Antiangiogenesis efficacy by TOP3 and IR combination treatment

Although the growth suppression by TOP3 alone was only temporary, the combination treatment resulted in significantly greater effect on the long-term suppression of tumor growth than IR alone (Figure 5). In order to resolve the discrepancy, the histological sections of HeLa/5HRE-Luc xenografts were examined on day 14 for an endothelial marker, CD31. As is clear from Figure 6a, CD31-positive microvessels distributed less in tumors with the combination treatment than those of other groups. Interestingly, TOP3 alone was effective in reducing the microvessels density (Figure 6a). The sections of HeLa/5HRE-Luc xenografts treated as Figure 5a were examined for the microvessel density (the number of microvessels per square millimeter) on day 14 after the initial treatments. The microvessel densities were 31.3 ± 9.5 and $28.5\pm10.0/mm^2$ for the control and IR-treated tumors, respectively which were not statistically different ($P=0.58$) (Figure 6b). In contrast, TOP3 treatment decreased the microvessel density to $17.5\pm3.7/mm^2$ with a good statistical significance ($P<0.001$). Moreover, the combination treatment of TOP3 and IR further reduced the density to $8.5\pm2.0/mm^2$ ($P<0.001$ over TOP3 treatment alone). Although there was a significant difference in the microvessel density between buffer- and TOP3-treated tumors on day 14 (Figures 6a and b), these two exhibited a similar speed of growth thereafter (Figures 5b and d). Immunohistochemical examination revealed that the buffer- and TOP3 alone did not differ in the microvessel density (Figure 6c), indicating anti-angiogenic function of TOP3 was temporary. In contrast, examination of the combination treatment demonstrated long lasting and statistically significant suppression of tumor neovascularizaiton in the tumor (Figure 6d; $P<0.01$ over TOP3 alone).

Discussion

It has long been recognized that the tumor hypoxia is a critical limit to radiotherapy. Various radiosensitizers have been developed in the past, which were designed to sensitize hypoxic tumor cells to radiation. However, their clinical use was hampered because of their neurotoxicity and low efficacy (Rowinsky, 1999; Zackrisson *et al*., 2003; Overgaard *et al*., 2005; Rischin *et al*., 2005). Recently, Sobhanifar *et al*. (2005) examined human tumor biopsies and human cancer xenografts with expression of HIF-1α and distribution of a chemical hypoxia marker, pimonidazole, which become reactive at less than 10 mm Hg oxygen tension. They found that expression of HIF-1α was reduced in the pimonidazole-positive regions, which are the target of the most of hypoxic cytotoxins. This suggests that these hypoxic cytotoxins are less effective in HIF-1-active hypoxic cells and may explain in part their low efficiency *in vivo*. HIF-1-active tumor cells have recently become a central issue for not only radiotherapy, but also for general tumor therapy since HIF-1 is now known to activate a variety of genes involved in anti-apoptosis and angiogenesis (Semenza, 2003).

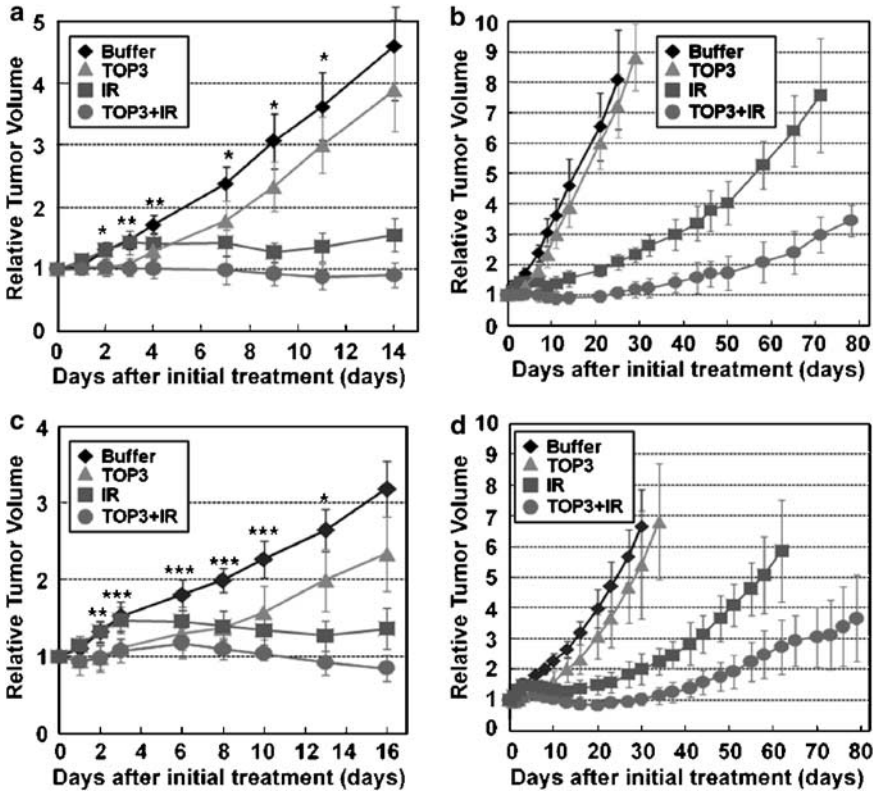

Figure 5 Antitumor effect induced by a combination of TAT-ODD-procaspase-3 (TOP3) and ionizing radiation (IR). Tumor-bearing mice ($n=10$ for each group) with HeLa/5HRE-Luc or CFPAC-1 xenografts in the right hind leg were treated as described in the legends to Figures 3 and 4; The mice of the TOP3 and the TOP3 and IR groups were treated with TOP3 on day 0, 1 and 2, and the mice of the IR and the TOP3 and IR groups were irradiated with 10 Gy on day 2. Tumor volume of HeLa/5HRE-Luc (**a** and **b**) and CFPAC-1 (**c** and **d**) xenografts treated as above were measured until day 78 and day 79, respectively. The relative tumor volume (the ratio of tumor volumes on each day to the corresponding ones on day 0) of HeLa/5HRE-Luc until day 14 (**a**) and day 78 (**b**) and the one of CFPAC-1 xenografts until day 16 (**c**) and day 79 (**d**) are presented in the graphs. The results are the mean of 10 independent tumors $\pm$ s.d. $^{*}P<0.05$; $^{**}P<0.01$; $^{***}P<0.001$ (none vs TOP3).

In this study, we treated tumors with the combination of IR and a hypoxia-targeting drug, TOP3. In monotherapy experiments, TOP3 temporarily suppressed tumor growth, but was not effective on long-term tumor growth inhibition (Figures 5b and d). Inhibition of HIF-1 by TOP3 was also temporary (Figures 3a and b). The combined treatment, however, resulted in significantly enhanced long-term suppression of tumor growth compared to either treatment alone (Figures 5b and d). Our results suggest that the enhanced effect of the combined treatment on long-term growth suppression (Figures 5b and d) was not simply due to an additive effect of TOP3 and IR on the tumor cells. We found that the microvessel density in the tumors treated with the combination was significantly reduced compared to either treatment alone in both short- and long-term-treated tumors (Figure 6). This result suggests that the enhanced growth suppression of the combination was due in part to the anti-angiogenic efficacy of the combined treatment. These results further indicate that the intratumoral HIF-1 activity is essential for the short-term restoration of damaged microvessels and long-term regrowth of irradiated tumors. Conversely, these results confirmed that hypoxia and its associated HIF-1 activity limit the efficacy of radiotherapy.

Recently, Moeller *et al.* (2004) demonstrated that irradiation of tumor xenografts with 5, 10 and 15 Gy induced HIF-1 activity, leading to the increased expression of VEGF and basic fibroblast growth factor, which act to prevent radiation-induced endothelial cell death. They also revealed that HIF-1 activity peaked at 48 h after radiation and provide evidence that radiation-induced reoxygenation of hypoxic tumor cells results in the production of reactive oxygen species (ROS) that induce HIF-1 activity. Our results are consistent with theirs: HIF-1 activity peaked at 2 days after IR (Figure 2) and suppression of HIF-1 activity resulted in reduced angiogenesis (Figures 6a and b) and significant enhancement of the tumor growth suppression by IR (Figures 5b and d).

Small molecules targeting HIF-1 have been developed which include 2-methoxyestradiol, 17-Allylamino-17-demethoxygeldanamycin, camptothecin, topotecan, pleurotin and YC-1. They inhibited HIF-1 activity and delayed tumor growth (Rapisarda *et al.*, 2002; de Candia *et al.*, 2003; Mabjeesh *et al.*, 2003; Semenza, 2003; Welsh *et al.*, 2003; Yeo *et al.*, 2003; Moeller *et al.*, 2004). In addition, novel inhibitors of signal transduction pathways were also observed to decrease the level of HIF-1α protein with resulting antiangiogenic effects

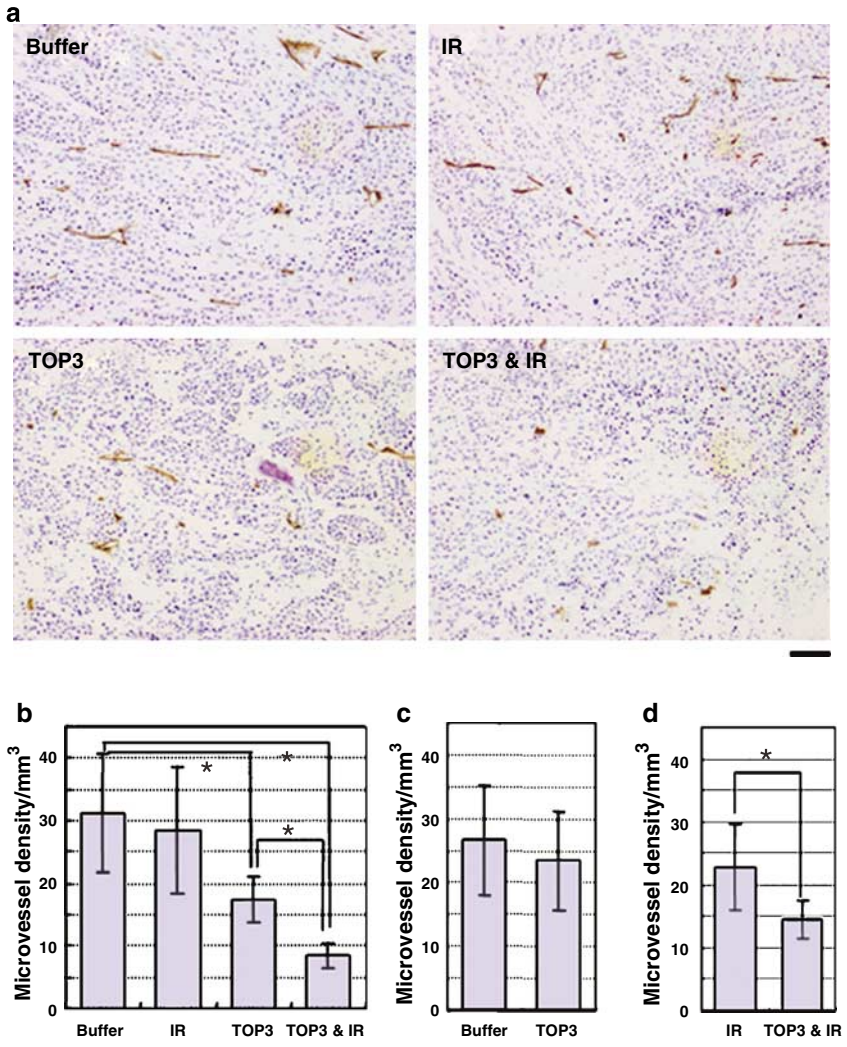

Figure 6 Inhibitory effect on tumor neovascularization induced by a combination of TAT-ODD-procaspase-3 (TOP3) and ionizing radiation (IR). (**a**) Tumor-bearing mice with HeLa/5HRE-Luc xenografts in the right hind leg were treated with buffer, TOP3, 10 Gy (IR) and TOP3 plus 10 Gy (TOP3 and IR) as described in the legend to Figure 5. The xenografts were surgically excised on day 14 and processed for immunohistochemical analysis with anti-CD31 antibody. A representative image of the tumor section in each treatment group is presented. Bar = 100 μm. (**b**) The number of the CD31-positive blood vessels per square millimeter (microvessel density/mm^3) in the section of the tumor on day 14 (Figure 6a) was counted under a microscope and the mean of 10 areas in three to four independent tumors for each treatment group is shown in the graph. (**c**) The xenografts from untreated (buffer) and TOP3-treated (TOP3) mice in Figure 5b were surgically excised on day 30 and analysed for their microvessel densities as Figure 6b legend. (**d**) The xenografts treated with 10 Gy (IR) or with both TOP3 and 10 Gy (TOP3 and IR) in Figure 5a were surgically excised on day 40 and analysed for microvessel density as described above. *$P<0.01$.

(Semenza, 2003). The mechanism of action of these small-molecule drugs has yet to be elucidated, and it is not known whether or not tumors develop resistance to them.

Our approach differs from small-molecule targeting of HIF-1. The small-molecules reduce HIF-1 activity, but do not kill the hypoxic cells. Therefore, these cells remain hypoxic and resistant to radiotherapy. In contrast, TOP3 kills HIF-1-active cells, which reside in the hypoxic region of the tumor and those arising during reoxygenation shortly after irradiation. Our approach reduces the problem of radioresistance of hypoxic cells and tumor regrowth stimulated by HIF-1-induced neovascularization.

HIF-1 is not the only hypoxia-regulating transcription factor in the cell. Other hypoxia-responsive factors such as HIF-2 are induced in hypoxic tumors, which are unlikely to be influenced by small-molecule HIF-1 inhibitors. In contrast, TOP3 kills all the hypoxic cells and therefore is a wider spectrum drug against hypoxic tumors. An additional possible advantage of TOP3 over small HIF-1 inhibitors is that its mechanism of action is clearly understood (Harada *et al*., 2006). TOP3 is activated only in HIF-1-active cells. If the tumors were to develop resistance to this newly developed drug, they would have to accumulate mutations, which inactivate the HIF-1 and prevent stabilization of HIF-1 in

hypoxia. This would result in the inability of tumors to induce neovascularization after therapy, which would prevent tumor regrowth.

In summary, we found in this study that TOP3 effectively eradicated HIF-1-active cells and as a consequence its application resulted in short-term suppression of angiogenesis in xenograft. This short-term anti-angiogenesis when combined with radiotherapy leads to long-term suppression of microvessels and total reduction of the hypoxic fraction in tumor xenograft.

Although we have been confirmed that stabilization itself does not endow TOP3 with cytocidal activity (Harada *et al*., 2006) and that TOP3 has not caused obvious side effects in animal experiments (Harada *et al*., 2002, 2005), as for the clinical application of a newly developed drug, the safety issue is the major concern. Since TOP3 eradicates HIF-1-active hypoxic cells, which are at the concentration far below their optimal oxygen concentration, its use in cancer patients with concomitant ischemic diseases may potentially pose a problem. In the case of ischemia however, the hypoxic condition is likely to be transient instead of permanent as in the case of tumors, and we still have no knowledge on how TOP3 affects such cells in a patient. In order to answer this important question, we have recently developed imaging probes, which detect such transient ischemia in a body by combining PTD, ODD and an imaging function domain (Tanaka *et al*., in preparation). With these probes in our hand, we are currently assessing the effect of TOP3 on transient ischemia in experimental systems.

Materials and methods

Cell culture and hypoxic treatment in vitro
The CFPAC-1 human pancreatic cancer cell line and HeLa human cervical epithelial adenocarcinoma cell line were purchased from the American Type Culture Collection. HeLa/EF-Luc and HeLa/5HRE-Luc that carry the luciferase reporter under control of the HIF promoter, were isolated as described previously (Harada *et al*., 2005). CFPAC-1 and HeLa cells were maintained at 37°C in 10% fetal bovine serum (FBS)–Iscove's modified Dulbecco's medium (Life Technologies, Inc., Rockville, MD, USA) and 5% FBS–Dulbecco's modified Eagle's medium (Nacalai Tesque, Kyoto, Japan), respectively.

Formulation of TOP3 fusion protein
TOP3 was dissolved in 10 mM Tris-HCl buffer (pH 8.0) at a final concentration of 15 μg/ml if not otherwise indicated.

Tumor model
HeLa/5HRE-Luc or CFPAC-1 cells were subcutaneously inoculated at 1×10^6 cells/100 μl of phosphate-buffered saline (PBS) into the right hind leg of 6-weeks-old female nude mice (BALB/c nu/nu; Japan SLC Inc., Hamamatsu, Japan). Day 0 was designated when tumors grew to approximately 200 mm^3 10 days after cell inoculation. These mice were then i.p. injected with TOP3 (20 mg/kg) on day 0, 1 and 2. Long-term monitoring of tumor growth was done by measuring the size of the tumors with calipers. Tumor volume was calculated as $0.5LW^2$.

Real-time monitoring of luciferase activity in vivo
Tumor-bearing mice were intravenously injected with 100 μl D-luciferin solution (10 mg/ml in PBS; Promega Corp., Madison, WI, USA). Exactly 3 min later, the mice were put in an IVIS-200 *in vivo* photon-counting device (Xenogen Corp., Alameda, CA, USA). The pseudo images from the photon counts were constructed by Living Image 2.50 – Igor Pro 4.09A software (Xenogen Corp.). Each image was quantified as photons/s and normalized against the day 0 photon counts. Each experimental group contained five mice.

Radiation treatment
Tumor-bearing mice were locally irradiated with 10 Gy of ^{137}Cs γ-ray using a collimator set at the tumor site with a Gammacell 40 Exactor (MDS Nordion International Inc., Ontario, Canada). The control tumor-bearing mice were sham irradiated.

Immunohistochemical analysis
Pimonidazole hydrochloride (60 mg/kg; Natural Pharmacia International Inc., Belmont, MA, USA) was i.p. injected into tumor-bearing mice at 90 min before surgical excision of solid tumors. The excised solid tumors were fixed in 10% formalin neutral buffer solution (pH 7.4; Wako Pure Chemical Industries Inc., Osaka, Japan) and embedded in paraffin. To detect pimonidazole-binding and luciferase proteins, serial sections prepared from the paraffin-embedded sections were treated with anti-pimonidazole (Natural Pharmacia International, Inc.) and anti-luciferase (Promega, Madison, WI, USA) antibodies, respectively. To detect CD31, surgically excised solid tumors were frozen in liquid N_2 and embedded in optimal cutting temperature (OCT). Sections prepared from the OCT-embedded tumor were treated with anti-CD31 antibody (BD Bioscience Pharmingen, San Diego, CA, USA). Staining was done with the indirect immunoperoxidase detection method (DakoCytomation, Carpinteria, CA, USA). Counter staining was done with hematoxylin. Paraffin-embedded serial sections were also stained with hematoxylin and eosin (H&E). Microvessel density was measured by counting the number of vessels (regions stained with anti-CD31 antibody) per square millimeter in each image.

Statistical analysis
Data are expressed as means $\pm$ s.d. Statistical significance of differences was determined by the paired two-tailed Student's *t*-test. Differences were considered statistically significant for $P < 0.05$.

Abbreviations

HIF-1, hypoxia-inducible factor-1; PTD, protein-transduction domain.

Acknowledgements

We are grateful to Dr Ohtsura Niwa for extensive discussion; Akiyo Morinibu, Emi Nishimoto and Naoko Harada for skilled technical assistance. This work was supported in part by grant-in-aid for Scientific Research on Priority Areas, Cancer, from the Ministry of Education, Culture, Sports, Science and Technology, and by a grant-in-aid for the second- and

third-Term Comprehensive 10-Year Strategy for Cancer Control from the Ministry of Health, Labor and Welfare, Japan. This study is a part of joint research, which is focusing on the development of the basis of technology for establishing COE for nano-medicine, carried out through Kyoto City Collaboration of Regional Entities for Advancing Technology Excellence (CREATE) assigned by Japan Science and Technology Agency (JST).

References

Abdollahi A, Lipson KE, Han X, Krempien R, Trinh T, Weber KJ *et al*. (2003). SU5416 and SU6668 attenuate the angiogenic effects of radiation-induced tumor cell growth factor production and amplify the direct anti-endothelial action of radiation *in vitro*. *Cancer Res* **63**: 3755–3763.

Brown JM. (1999). The hypoxic cell: a target for selective cancer therapy – eighteenth Bruce F. Cain Memorial Award lecture. *Cancer Res* **59**: 5863–5870.

Brown JM, Wilson WR. (2004). Exploiting tumor hypoxia in cancer treatment. *Nat Rev Cancer* **4**: 437–447.

Bruick RK, McKnight SL. (2001). A conserved family of prolyl-4-hydroxylases that modify HIF. *Science* **294**: 1337–1340.

Cockman ME, Masson N, Mole DR, Jaakkola P, Chang GW, Clifford SC *et al*. (2000). Hypoxia inducible factor-alpha binding and ubiquitylation by the von Hippel–Lindau tumor suppressor protein. *J Biol Chem* **275**: 25733–25741.

de Candia P, Solit DB, Giri D, Brogi E, Siegel PM, Olshen AB *et al*. (2003). Angiogenesis impairment in Id-deficient mice cooperates with an Hsp90 inhibitor to completely suppress HER2/neu-dependent breast tumors. *Proc Natl Acad Sci USA* **100**: 12337–12342.

Epstein AC, Gleadle JM, McNeill LA, Hewitson KS, O'Rourke J, Mole DR *et al*. (2001). *C. elegans* EGL-9 and mammalian homologs define a family of dioxygenases that regulate HIF by prolyl hydroxylation. *Cell* **107**: 43–54.

Fernandes-Alnemri T, Litwack G, Alnemri ES. (1994). CPP32, a novel human apoptotic protein with homology toaenorhabditis elegans cell death protein Ced-3 and mammalian interleukin-1 beta-converting enzyme. *J Biol Chem* **269**: 30761–30764.

Geng L, Donnelly E, McMahon G, Lin PC, Sierra-Rivera E, Oshinka H *et al*. (2001). Inhibition of vascular endothelial growth factor receptor signaling leads to reversal of tumor resistance to radiotherapy. *Cancer Res* **61**: 2413–2419.

Gorski DH, Beckett MA, Jaskowiak NT, Calvin DP, Mauceri HJ, Salloum RM *et al*. (1999). Blockage of the vascular endothelial growth factor stress response increases the antitumor effects of ionizing radiation. *Cancer Res* **59**: 3374–3378.

Harada H, Hiraoka M, Kizaka-Kondoh S. (2002). Antitumor effect of TAT-oxygen-dependent degradation-caspase-3 fusion protein specifically stabilized and activated in hypoxic tumor cells. *Cancer Res* **62**: 2013–2018.

Harada H, Kizaka-Kondoh S, Hiraoka M. (2005). Optical imaging of tumor hypoxia and evaluation of efficacy of a hypoxia-targeting drug in living animals. *Mol Imaging* **4**: 182–193.

Harada H, Kizaka-Kondoh S, Hiraoka M. (2006). Mechanism of hypoxia-specific cytotoxicity of procaspase-3 fused with a VHL-mediated protein destruction motif of HIF-1a containing Pro564. *FEBS Lett* **580**: 5718–5722.

Harris AL. (2002). Hypoxia-a key regulatory factor in tumour growth. *Nat Rev Cancer* **2**: 38–47.

Höckel M, Knoop C, Schlenger K, Vorndran B, Baussmann E, Mitze M *et al*. (1993). Intratumoral pO_2 predicts survival in advanced cancer of the uterine cervix. *Radiother Oncol* **26**: 45–50.

Huang LE, Gu J, Schau M, Bunn HF. (1998). Regulation of hypoxia-inducible factor 1 alpha is mediated by an O2-dependent degradation domain via the ubiquitin-proteasome pathway. *Proc Natl Acad Sci USA* **95**: 7987–7992.

Inoue M, Mukai M, Hamanaka Y, Tatsuta M, Hiraoka M, Kizaka-Kondoh S. (2004). Targeting hypoxic cancer cells with a protein prodrug is effective in experimental malignant ascites. *Int J Oncol* **25**: 713–720.

Kallio PJ, Wilson WJ, O'Brien S, Makino Y, Poellinger L. (1999). Regulation of the hypoxia-inducible transcription factor 1alpha by the ubiquitin-proteasome pathway. *J Biol Chem* **274**: 6519–6525.

Kamura T, Sato S, Iwai K, Czyzyk-Krzeska M, Conaway RC, Conaway JW. (2000). Activation of HIF1alpha ubiquitination by a reconstituted von Hippel–Lindau (VHL) tumor suppressor complex. *Proc Natl Acad Sci USA* **97**: 10430–10435.

Kizaka-Kondoh S, Inoue M, Harada H, Hiraoka M. (2003). Tumor hypoxia: a target for selective cancer therapy. *Cancer Sci* **94**: 1021–1028.

Mabjeesh NJ, Escuin D, LaVallee TM, Pribluda VS, Swartz GM, Johnson MS *et al*. (2003). 2ME2 inhibits tumor growth and angiogenesis by disrupting microtubules and dysregulating HIF. *Cancer Cell* **3**: 363–375.

Moeller BJ, Cao Y, Li CY, Dewhirst MW. (2004). Radiation activates HIF-1 to regulate vascular radiosensitivity in tumors: role of reoxygenation, free radicals, and stress granules. *Cancer Cell* **5**: 429–441.

Ohh M, Park CW, Ivan M, Hoffman MA, Kim TY, Huang LE *et al*. (2000). Ubiquitination of hypoxia-inducible factor requires direct binding to the beta-domain of the von Hippel–Lindau protein. *Nat Cell Biol* **2**: 423–427.

Overgaard J, Eriksen JG, Nordsmark M, Alsner J, Horsman MR, Danish Head and Neck Cancer Study Group. (2005). Plasma osteopontin, hypoxia, and response to the hypoxia sensitiser nimorazole in radiotherapy of head and neck cancer: results from the DAHANCA 5 randomised double-blind placebo-controlled trial. *Lancet Oncol* **6**: 757–764.

Raleigh JA, Calkins-Adams DP, Rinker LH, Ballenger CA, Weissler MC, Fowler Jr WC *et al*. (1998). Hypoxia and vascular endothelial growth factor expression in human squamous cell carcinomas using pimonidazole as a hypoxia marker. *Cancer Res* **58**: 3765–3768.

Rapisarda A, Uranchimeg B, Scudiero DA, Selby M, Sausville EA, Shoemaker RH *et al*. (2002). Identification of small molecule inhibitors of hypoxia-inducible factor 1 transcriptional activation pathway. *Cancer Res* **62**: 4316–4324.

Rischin D, Peters L, Fisher R, Macann A, Denham J, Poulsen M *et al*. (2005). Tirapazamine, Cisplatin, and radiation versus fluorouracil, cisplatin, and radiation in patients with locally advanced head and neck cancer: a randomized phase II trial of the Trans-Tasman Radiation Oncology Group (TROG 98.02). *J Clin Oncol* **23**: 79–87.

Rowinsky EK. (1999). Novel radiation sensitizers targeting tissue hypoxia. *Oncology* **13**: 61–70.

Schwarze SR, Ho A, Vocero-Akbani A, Dowdy SF. (1999). *In vivo* protein transduction: delivery of a biologically active protein into the mouse. *Science* **285**: 1569–1572.

Semenza GL. (2003). Targeting HIF-1 for cancer therapy. *Nat Rev Cancer* **3**: 721–732.

Semenza GL, Wang GL. (1992). A nuclear factor induced by hypoxia via *de novo* protein synthesis binds to the human

erythropoietin gene enhancer at a site required for transcriptional activation. *Mol Cell Biol* **12**: 5447–5454.

Sobhanifar S, Aquino-Parsons C, Stanbridge EJ, Olive P. (2005). Reduced expression of hypoxia-inducible factor-1alpha in perinecrotic regions of solid tumors. *Cancer Res* **65**: 7259–7266.

Tanimoto K, Makino Y, Pereira T, Poellinger L. (2000). Mechanism of regulation of the hypoxia-inducible factor-1 alpha by the von Hippel–Lindau tumor suppressor protein. *EMBO J* **19**: 4298–4309.

Vaupel P. (2001). Tumor microenvironmental physiology and its implications for radiation oncology. *Semin Radiat Oncol* **14**: 198–206.

Vaupel P, Kallinowski F, Okunieff P. (1989). Blood flow, oxygen and nutrient supply, and metabolic microenvironment of human tumors: a review. *Cancer Res* **49**: 6449–6465.

Welsh SJ, Williams RR, Birmingham A, Newman DJ, Kirkpatrick DL, Powis G. (2003). The thioredoxin redox inhibitors 1-methylpropyl 2-imidazolyl disulfide and pleurotin inhibit hypoxia-induced factor 1alpha and vascular endothelial growth factor formation. *Mol Cancer Ther* **2**: 235–243.

Yeo EJ, Chun YS, Cho YS, Kim J, Lee JC, Kim MS *et al*. (2003). YC-1: a potential anticancer drug targeting hypoxia-inducible factor 1. *J Natl Cancer Inst* **95**: 516–525.

Zackrisson B, Mercke C, Strander H, Wennerberg J, Cavallin-Stahl E. (2003). A systematic overview of radiation therapy effects in head and neck cancer. *Acta Oncol* **42**: 443–461.